

The C_ℓOVER Experiment

L. Piccirillo¹, P. Ade², M. D. Audley³, C. Baines¹, R. Battye¹, M. Brown³, P. Calisse², A. Challinor^{5,6}, W. D. Duncan⁷, P. Ferreira⁴, W. Gear², D. M. Glowacka³, D. Goldie³, P.K. Grimes⁴, M. Halpern⁸, V. Haynes¹, G. C. Hilton⁷, K. D. Irwin⁷, B. Johnson⁴, M. Jones⁴, A. Lasenby³, P. Leahy¹, J. Leech⁴, S. Lewis¹, B. Maffei¹, L. Martinis¹, P. D. Mauskopf², S. J. Melhuish¹, C. E. North⁴, D. O'Dea³, S. Parsley², G. Pisano¹, C. D. Reintsema⁷, G. Savini², R.V. Sudiwala², D. Sutton⁴, A. Taylor⁴, G. Teleberg², D. Titterington³, V. N. Tsaneva³, C. Tucker², R. Watson¹, S. Withington³, G. Yassin⁴, J. Zhang²

¹ *School of Physics and Astronomy, University of Manchester, UK*

² *School of Physics and Astronomy, Cardiff University, UK*

³ *Cavendish Laboratory, University of Cambridge, Cambridge, UK*

⁴ *Astrophysics, University of Oxford, Oxford, UK*

⁵ *Institute of Astronomy, University of Cambridge, Cambridge, UK*

⁶ *DAMTP, University of Cambridge, Cambridge, UK*

⁷ *National Institute of Standards and Technology, USA*

⁸ *University of British Columbia, Canada*

C_ℓOVER is a multi-frequency experiment optimised to measure the Cosmic Microwave Background (CMB) polarization, in particular the B-mode component. C_ℓOVER comprises two instruments observing respectively at 97 GHz and 150/225 GHz. The focal plane of both instruments consists of an array of corrugated feed-horns coupled to TES detectors cooled at 100 mK. The primary science goal of C_ℓOVER is to be sensitive to gravitational waves down to $r \sim 0.03$ (at 3σ) in two years of operations.

1 Introduction

The Cosmic Microwave Background (CMB) Radiation is a very powerful tool to study the origin and evolution of the Universe. The CMB initial fluctuations are connected with the physics of the early Universe. The study of these fluctuations will help in understanding this physics at a time when the energy scale was plausibly of the order of 10^{16} GeV. The CMB is

linearly polarized by Thomson scattering around the time of recombination. In the same way that a vector field can be written as the gradient of a scalar field and a divergence-free vector field, the spin-2 CMB polarization can be decomposed into a gradient-like term (denoted the E mode due to its electric parity) and a curl-like mode (denoted B due to its magnetic parity). Given a sky map of the Q and U Stokes local parameters, it is then possible to generate two maps representing respectively the E and B-modes of the CMB polarization. The decomposition leading to these maps is very interesting because, due to their symmetry, linear density perturbations cannot generate B-modes. Large-angular scales B-modes are generated by primordial gravity waves with wavelengths of the order of the horizon at the time of recombination. The detection and characterization of these B-modes will represent a fantastic tool to probe this extraordinary period in the history of the Universe. Constraints on gravitational waves are usually quoted in terms of the tensor-to-scalar ratio of primordial amplitudes, $r \sim A_t/A_s$. The current 95% constraint is $r < 0.20$ (Hinshaw et al. 2008). This corresponds to an energy scale $V^{1/4} < 2.4 \times 10^{16}$ GeV, close to that expected in models based on Grand Unified Physics.

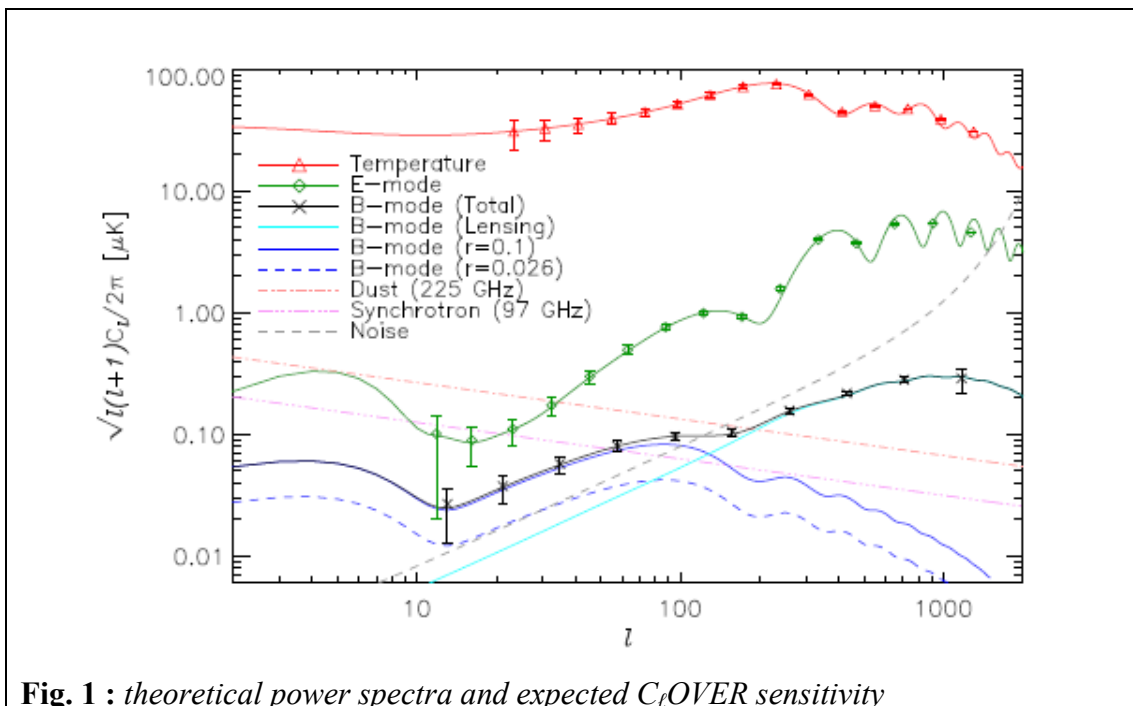


Fig. 1 : *theoretical power spectra and expected C_l OVER sensitivity*

The theoretical angular power spectra for the temperature, E-mode and B-mode signals assuming the Λ CDM cosmological model and $r = 0.1$ are shown in fig. 1. The black, B-mode curve comprises a primordial inflationary gravity wave signal and a predicted non-primordial B-mode secondary signal produced by the gravitational lensing of partially polarised CMB radiation as it passed through large-scale structures. The expected performance of C_l OVER is over-plotted as binned points, with error bars taking into account the atmospheric and instrumental noise for 150GHz and the sample variance for the C_l OVER survey area. For comparison, we plot the power spectra of the forecasted foreground signals in the C_l OVER

observation regions before cleaning, based on polarization observations and models of unpolarized emission. These foreground signals include polarized thermal emission from aligned dust grains and polarized synchrotron emission. The dust and synchrotron signals are plotted at 225 and 97GHz, respectively, to show the worst case scenario. For a more detailed description of C_t OVER sensitivity together with the observing strategy, see North et al., (2008).

2 The design parameters

The CMB anisotropy has been very well characterized by a series of successful experiments from the ground, balloon and space-born. Today we have high confidence that the CMB

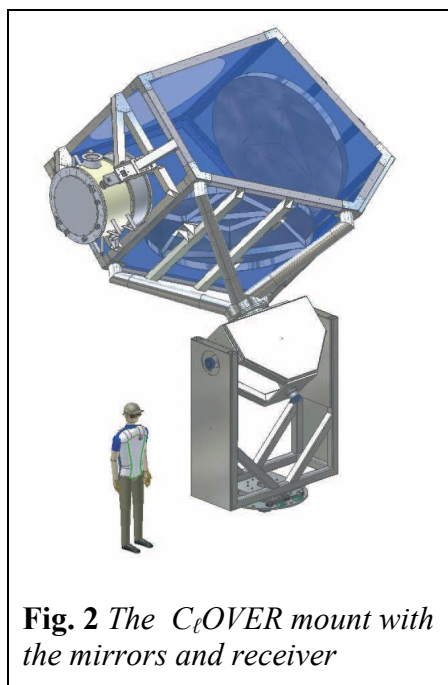


Fig. 2 The C_t OVER mount with the mirrors and receiver

anisotropy fluctuations have an *rms* value of the order of 100 μ K. The expected *rms* fluctuation amplitude in the sky for the CMB polarization

fluctuations (E-mode) is around 6 μ K. The E-modes are now being characterized with some accuracy by several experiments: WMAP (Kogut et al., 2003; Page et al. 2007; Nolte et al. 2008), DASI (Kovac et al. 2002; Leitch et al. 2005), CBI (Readhead et al. 2004; Sievers et al. 2007), BOOMERanG (Montroy et al. 2006), Maxipol (Wu et al. 2007) and very recently QuAD (Ade et al., 2008). The current limit, $r < 0.2$, from combining CMB temperature measurements with distance measures from supernovae and the baryon acoustic oscillation feature in the clustering of galaxies implies that the primordial B-mode signal is at most a few 100 nK. Such an extraordinary low signal level needs to be taken into account when designing new instruments. In particular, in addition to raw sensitivity – which can be achieved by using large format arrays as well as background limited detectors – we need to pay attention to potential

systematic effects in our instrument that can easily mimic the signal we are after. A considerable amount of time and effort has been dedicated by our team to the design of the C_t OVER instrument in all its individual sub-systems – like, for

example the corrugated feed-horns, the OMTs or the Half-Wave-Plates. We performed a series of simulations that provided us with technical specifications for each of the sub-systems for each systematic effect considered (for example cross-polarization, instrumental polarization, depolarization and beam ellipticity). For a more in-depth treatment, see O’Dea

Cross - Polarization	< -47 dB
Polarimeter efficiency	> 90%
Instrumental Polarization	< 0.02%

Table 1: Acceptable levels of systematic error for C_t OVER. One can interpret these values as fabrication requirements or a threshold to which each error must be subtracted during data analysis.

et al., 2007. Once the specifications were fixed, we proceeded to build and characterize all the C_tOVER subsystems.

	97 GHz	150 GHz	225 GHz
NEP _{ph} atmo (10^{-17} W/ $\sqrt{\text{Hz}}$)	1.76	3.35	5.97
NEP _{ph} mirrors (10^{-17} W/ $\sqrt{\text{Hz}}$)	0.940	1.38	1.73
NEP _{ph} cryo window (10^{-17} W/ $\sqrt{\text{Hz}}$)	0.951	1.40	1.75
NEP _{ph} CMB (10^{-17} W/ $\sqrt{\text{Hz}}$)	0.522	0.563	0.436
Total NEP (10^{-17} W/ $\sqrt{\text{Hz}}$)	2.61	4.51	8.03
Total NET ($\mu\text{K } \sqrt{\text{sec}}$)	124	189	524

Table 2: various contributions to the NEP (NET)

NEP and NET: The Noise Equivalent Power of C_tOVER receivers at 97, 150 and 225 GHz must be estimated taking into account all potential sources of noise. Our estimates assume an overall optical efficiency of 50%, a telescope temperature and emissivity of respectively 275K and 2%, a cryostat window temperature and emissivity of respectively 275K and 1%. In spite of a site choice with favorable atmospheric conditions (Pampa la Bola, Atacama desert at 5080 m. altitude), we expect the spurious signal generated by atmospheric emission and fluctuations to be well above the intrinsic instrumental noise. Our estimates of atmospheric emission rely on a fiducial atmospheric transmission model and 225 GHz τ values measured at Atacama by the ALMA collaboration (Otarola et al., 2005). The following table lists the estimates of instrumental NEPs including the atmospheric emission evaluated for average observing elevation angles around 60 degrees. In the total NEP estimate we included a detector NEP equal to the overall instrumental NEP.

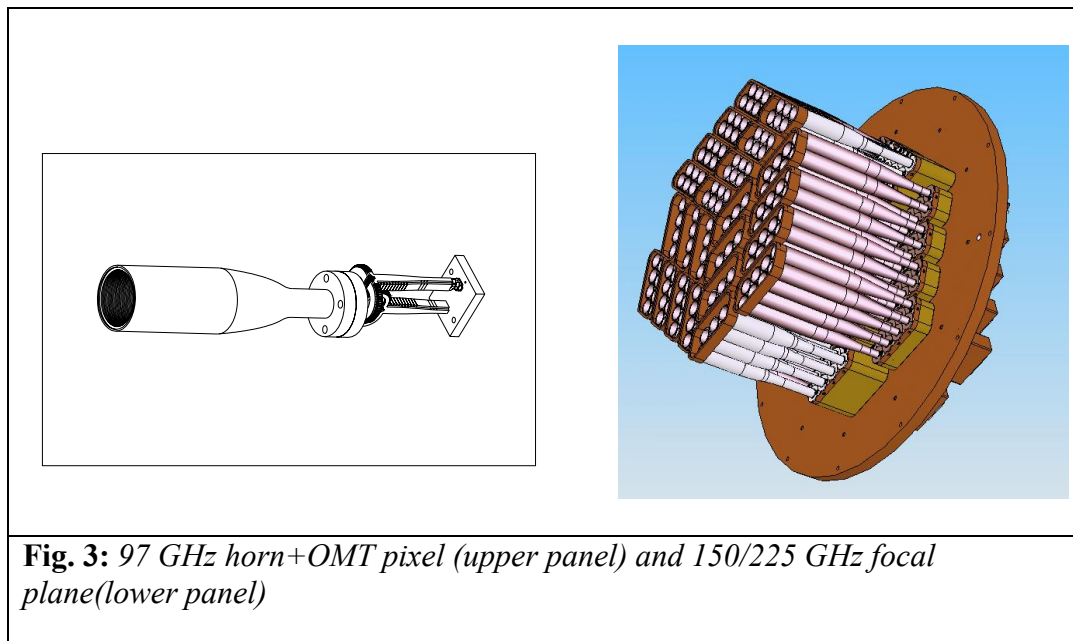


Fig. 3: 97 GHz horn+OMT pixel (upper panel) and 150/225 GHz focal plane (lower panel)

3 The C_lOVER instrument

The main drivers for the design of C_lOVER have been the minimization of the major potential sources systematic effects and the achievement of the required sensitivity. The instrument is composed of two identical 3-axial mounts (see left picture). The first mount (LF instrument) contains the 97 GHz receiver coupled to the optical assembly; the second mount (HF instrument) contains the 150/225 GHz instrument coupled to an identical optical assembly. The 3-axial mount is capable of the full range of azimuth and elevation motions. The addition of the third axis (z-rotation) will allow us to rotate the instruments around the observing direction. The optical assembly has a design that is common to the two instruments and uses a Compact Range Antenna (CRA) design. The C_lOVER CRA is composed of a parabolic off-axis primary mirror and a hyperbolic off-axis secondary mirror. This optical design gives excellent optical performances across a large, flat focal plane. For all focal plane elements, the Strehl ratio is greater than 0.95, and the cross-polarisation – including the cross polarisation of the horn – is better than -38 dB. The projected diameters of the primary mirrors are 1.8 and 1.5 meters for the 97 and 150/225 GHz instruments respectively. The telescope mirrors will be surrounded by a co-moving baffle lined with millimetre-wave absorber, which will prevent polarized signals in the far side lobes of the telescope from being modulated as the telescope scans. The secondary mirror of each instrument will be under illuminated to reduce the total spill-over to a value of about 1%. In this way, the total power on the detector coming from the emission of the co-moving absorbing baffle will be 25% of the total power received resulting in a negligible contribution to the total NEP. The focal plane is composed of an array of polarimeters. Each polarimeter is composed of a profiled corrugated single-mode feed-horn which defines a Gaussian beam in the sky. The beams are 7.5 arcmin for the 97 GHz instrument and 5.5 arcmin for the 150/225 GHz instrument.

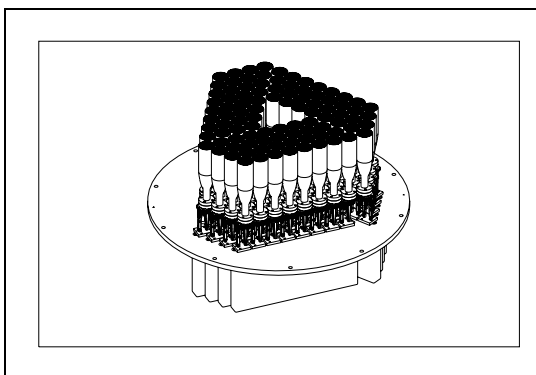


Fig. 4: 97 GHz focal plane array showing the 96 profiled corrugated feed-horns, the OMTs, the 100 mK baseplate and, on the back, the TES detector blocks

Polarimetry: the 97 GHz polarimeter pixel is composed of a combination of corrugated feed-horn plus OMT. The OMT is composed of an electroformed turnstile junction with a circular waveguide input and two rectangular waveguide outputs (Pisano G. et al., 2007). Each waveguide will carry the two polarized components (vertical and horizontal) of the input radiation (see fig on the left). The RF power in each of the waveguide is coupled to a superconductive micro-strip line – by means of a tapered finline – and then terminated into a 20 Ω resistor thermally coupled to the TES detector. The 150/225 GHz polarimeter pixel is designed differently: the output circular waveguide of the corrugated feed-horn is coupled to a planar 4-probe OMT realized on the same substrate where the TES detectors are. As in the case of the 97 GHz, two TES

detectors will receive the RF power coming from respectively the vertical and horizontal polarized component of the RF input power. The fig. on the left shows the 150/225 GHz focal plane array concept. Detector drifts and atmospheric fluctuations will introduce $1/f$ noise into our data. To reject systematic errors and to achieve the best noise performance, C_tOVER will use rapid polarization modulation. This modulation is produced by a rotating achromatic half-wave plate (HWP) and fixed OMT transducers, which are the polarization analyzers. The 97 GHz HWP will be operated at room temperature and position in front of the cryostat window. The 150/225 GHz HWP will be at cryogenic temperature inside the cryostat.

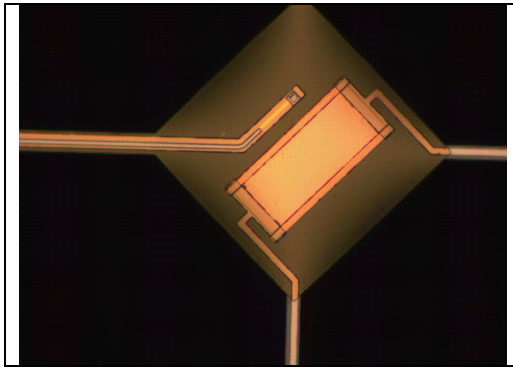


Fig. 5: TES detector for the 97 GHz instrument

The detectors: C_tOVER uses TES detectors at all its observing frequencies (97, 150 and 225 GHz). Members of our group have developed all the technology for the successful fabrication and testing of the C_tOVER TES detectors (see, for example, Glowacka et al., 2008). Transition Edge Superconductors offer high sensitivity, with noise equivalent powers of around 10^{-17} WHz^{-1/2}, wide RF bandwidths, typically 50 GHz, and good saturation powers, typically 20 to 100 pW. Our microstrip-coupled TES consists of a superconducting bilayer (Mo/Cu) deposited on a silicon nitride membrane, which is thermally

isolated by thin legs. The RF power coming from the waveguide at the output of the OMT is coupled to the microstrip (Audley et al, 2006). The RF power in the microstrip is then coupled to the membrane through a thin-film superconducting transmission line terminated by a resistor. For maximum sensitivity, we require that the detectors be background-limited, i.e. the contributions to the noise equivalent power (NEP) from the detectors and readout must be less than half of the photon noise from the sky.

Once the detectors are background-limited the only way to improve the sensitivity is to increase the number of detectors. In addition to low noise, C_tOVER detectors must have a time constant less than 1 ms and must be able to absorb the power incident from the sky without saturation. This power is variable and depends on the weather. The power-handling requirement is for the detectors to be able to operate for 75% of the time at the site. We require that the detectors will not saturate with RF powers up to 6.7, 11.5 and 18.8 pW for respectively the 97, 150 and 225 GHz channels. Prototypes of the 97 GHz detectors have been built and tested. We verified that the measured performances are consistent with the design parameters. In particular we achieved a very high optical efficiency (>90%).

The cryogenics: The main task of the two C_tOVER cryostats will be to cool the two focal plane polarimeters and TES detectors to the required operating temperatures. The 97 GHz cryostat has been built and it is currently undergoing the AIV phase. The 150/225 GHz cryostat has an almost identical design because of the similar TES operating temperatures and masses to be cooled. In the following we restrict the cryogenics description to the 97 GHz cryostat mostly because it has been already built and tested and therefore is in a more advanced state. The C_tOVER 97 GHz cryostat consists of the following elements:

- A modular vacuum can with optical window, signal and housekeeping readout vacuum connectors and PTC flange
- A Pulse Tube Cooler (model Cryomech PT410) providing about 30W of cooling power at 40K and 1W of cooling power at 4K;
- A series of radiation shields at various temperatures (40K, 3K, 1.5K, 300 mK) cooling mainly the optical filters;
- A He-7 closed-cycle sorption fridge to provide 1.5K and 300 mK base temperatures (with respectively 5 mW and 100 μ W cooling power) to operate the dilution fridge;
- A miniature closed-cycle dilution refrigerator (mini-DR) to provide 800 mK and 80 mK temperature (with respectively 1 mW and 3 μ W cooling power) to cool the detectors;
- A series of thermal straps and isolation stages
- A 3K to 100 mK support structure mechanically holding the weight of the focal planes (\sim 15 Kg). This structure will isolate thermally the focal plane, at about 100 mK, from the 2nd stage baseplate temperature at about 3K.

The 97GHz cryostat has been designed and built with the following goals:

- Cool the TES detector blocks at 80 mK. Keep this temperature constant within the specifications ($\delta T_{\text{rms}} \cong 10$ nK);
- Keep the TES detector blocks at 80 mK for 12 hours or more;
- Provide the 3.5 K baseplate temperature to operate the service He-7 fridge (FHM), cool the inner 3K radiation shields and 3 K filters;
- Provide the 40K baseplate temperature to cool the inner 40K radiation shields and the 40K filters;

In addition, the 97GHz cryostat provides:

- Low level of thermal and mechanical fluctuations together with a low level of Radio Frequency Interference;
- Easy accessibility to the focal plane hardware and cryogenics;
- Rapid cool-down time;
- Simple assembly/disassembly procedure;
- Simple cabling providing easy replacement in case of failures;

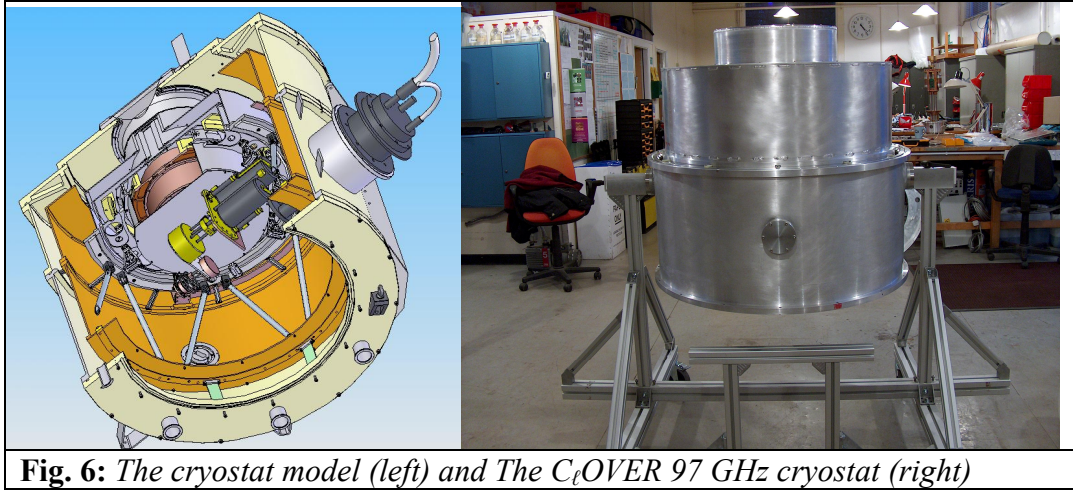


Fig. 6: *The cryostat model (left) and The C_iOVER 97 GHz cryostat (right)*

The final 100 mK temperature is achieved by a cascade of closed-cycle refrigerators: the Cryomech PTC 410, the Chase Research He-7 FHM, the mini dilution refrigerator built in collaboration with Chase Research.

300K → 45K (1st stage of the PT410):	T = 45K with Input Power = 27W
45K → 3.5K (2nd stage of the PT410):	T = 3.5K with Input Power = 314 mW
3.5K → 2K (FHM gas cooled stage):	T = 2.0K with Input Power = 279 μW
2K → 0.7K (mini-DR still):	T = 0.7K with Input Power = 63 μW
0.7K → 0.4K (FHM cold plate):	T = 0.4K with Input Power = 204 μW
0.4K → 0.1K (mini-DR mixing chamber):	T = 0.1K with Input Power = 2.4 μW

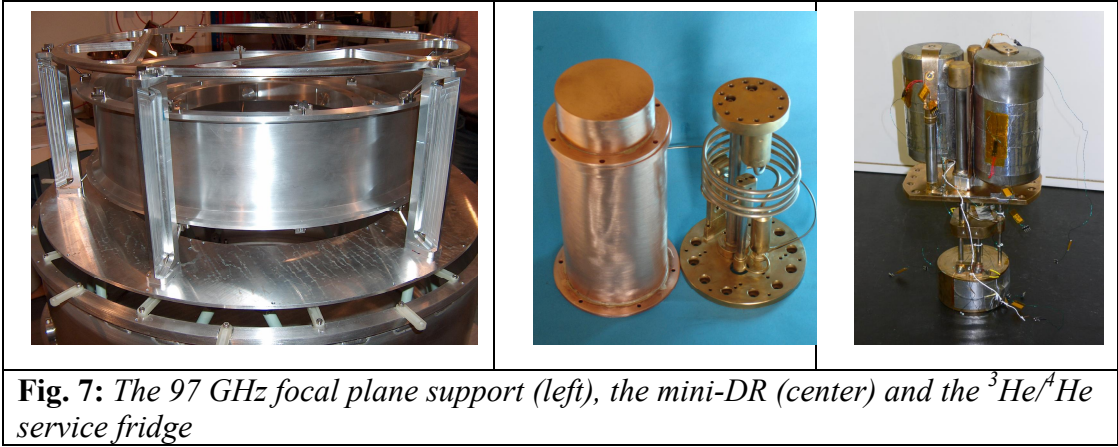


Fig. 7: *The 97 GHz focal plane support (left), the mini-DR (center) and the ³He/⁴He service fridge*

The available cooling power at each stage is:

1st stage PTC410:	30W
2nd stage PTC410:	500 mW
FHM gas cooled stage:	279 μW
mini-DR still:	200 μW

FHM cold plate: 250 μ W
mini-DR mixing chamber: 3 μ W

The cryogenics is one of the most difficult and challenging part of this experiment and required many novel solutions. Here is a partial list of the solutions adopted:

- The sub-K cryogenics chain consists of a double stage $^3\text{He}/^4\text{He}$ to provide a temperature of about 350 mK with 200 μ W cooling power. The first double stage $^3\text{He}/^4\text{He}$ was built by members of our collaboration (Dall'Oglio et al., 1991).
- The 100 mK temperature is achieved by means of a miniature dilution refrigerator designed and built by members of our collaborations (Teleberg G. et al., 2008).
- A novel tiltable mini-DR has been designed and built by us capable of work under 45° tilt. This is the only dilutor with this characteristics, to the best of our knowledge (Piccirillo L. et al., 2008)
- The thermal isolation and mechanical support from 0.7K to 300 mK and from 300 mK to 100 mK is achieved with novel sapphire supports.
- The TES detectors are tested with a test cryostat built to test all the concept of the C_tOVER final cryostats. It is composed of exactly the same chain: PTC, double stage $^3\text{He}/^4\text{He}$ and mini-DR.
- The test cryostat achieves routinely 70 mK base temperature and contains the magnetic shielding capable of reaching the lowest NEPs.

4 Conclusions

C_tOVER is an instrument designed to measure the B-modes in the CMB polarization. The very small signal levels expected impose a careful detailed design of the system to minimise – or keep under control – systematic effects. In the course of our effort to design C_tOVER we needed to introduce several new technical and scientific novelties, like for example the Compact Range Antenna optical configuration, the profiled corrugated feed horns, the electroformed or planar OMTs, the TES detectors, the cryogenics, etc. We believe that all these novel technical solutions will help the design of the current and future B-mode experiments.

5 References

- [1] Ade et al., The Astrophysical Journal, Volume 674, Issue 1, pp. 22-28, (2008)
- [2] Audley M. D. et al., Proceedings of the SPIE, Volume 6275, pp. 627524 (2006)
- [3] Dall'Oglio G., Pizzo L., Piccirillo L. and Martinis L., Cryogenics, vol. 31, Jan. 1991, p. 61-63
- [4] Kogut A. et al., 2003, ApJS, 148, 161
- [5] Kovac J. M., Leitch E. M., Pryke C., Carlstrom J. E., Halverson N. W., Holzappel [6] W. L., 2002, Nature, 420, 772

- [7] Lewis A., Challinor A., Turok N., 2002, Phys. Rev. D, 65, 023505
- [8] Glowacka D.M. et al., J. Low Temp. Phys. (2008) 151: 249–254
- [9] Montroy T. E. et al., 2006, ApJ, 647, 813
- [10] North C. E., et al, eprint arXiv:0805.3690
- [11] O’Dea, D., Challinor, A., and Johnson, B. R. (2007) MNRAS 376(4), 1767
- [12] Otarola, A., et al. 2005. “ALMA Memo #512. Atmospheric Transparency at Chajnantor; 1973-2003.”
- [13] Page et al. The Astrophysical Journal Supplement Series, Volume 170, Issue 2, pp. 335-376 (2007)
- [14] Piccirillo L., et al, in preparation (2008)
- [15] Pietranera L. et al., Monthly Notices of the Royal Astronomical Society, Volume 376, Issue 2, pp. 645-650, 2007
- [16] Pisano, G. et al. (2007) IEEE Microwave Compon. Lett. 17(4), 28
- [17] Hinshaw, G. et al. (2008) ApJS submitted, astro-ph/0803.0732
- [18] Readhead A. C. S. et al., 2004, Science, 306, 836
- [19] Sievers et al., The Astrophysical Journal, Volume 660, Issue 2, pp. 976-987 (2007)
- [20] Teleberg G., Chase S. and Piccirillo L., Journal of Low Temperature Physics, Volume 151, Issue 3-4, pp. 669-674, 2008
- [21] Wu et al., The Astrophysical Journal, Volume 665, Issue 1, pp. 55-66, 2007